European Polymer Journal 121 (2019) 109311

Contents lists available at ScienceDirect

European Polymer Journal

journal homepage: www.elsevier.com/locate/europolj

Insights in the Ni-thiophene association in the synthesis of thiophene-*para*-phenylene block copolymers via Kumada catalyst transfer condensative polymerization

Ward Ceunen[a], Julien De Winter[b], Pascal Gerbaux[b], Guy Koeckelberghs[a,*]

[a] Laboratory for Polymer Synthesis, Department of Chemistry, KU Leuven, Celestijnenlaan 200F, 3001 Heverlee, Belgium
[b] Organic Synthesis and Mass Spectrometry Laboratory, Interdisciplinary Center for Mass Spectrometry, University of Mons-UMONS, 23 Place du Parc, 7000 Mons, Belgium

ARTICLE INFO

Keywords:
Conjugated polymers
KCTCP
External Ni-initiators

ABSTRACT

In this article we investigate association of the Ni-catalyst during Kumada catalyst transfer condensative polymerization (KCTCP) and hypothesize that when adding a *para*-phenylene monomer to a living thiophene block to synthesize poly(thiophene)-*b*-poly(*para*-phenylene), an equilibrium exist between the incorporation of the *para*-phenylene monomer and the trapping of the Ni-catalyst by association with the thiophene block. We suggest that this equilibrium shifts toward the association with the thiophene block with increasing length of the thiophene block and that significant trapping only occurs when this block consist of several thiophene units.

1. Introduction

The interesting opto-electronic properties of conjugated polymers make them promising lightweight and easy-to-process materials to be used in advanced applications such as organic electronics, photovoltaic solar cells, transistor devices, electrochemical capacitors, chemical and biological sensors, light emission, charge transport and photocatalytic H_2 generation [1–20]. Within this class of materials, poly(thiophene)s are the most studied due to their good environmental and thermal stability, processability and the availability of an extensive toolbox for their controlled synthesis [21–26]. This control over the polymerization is crucial for the production of tailor made high-end materials with predictable molar masses, low dispersities, control over the end-groups and regularity, which have all shown to strongly affect the performance of these materials [27,28]. Furthermore, a controlled block copolymerization by sequential monomer addition can lead to new morphologies and advanced well-defined materials for specific applications [29–32].

For poly(thiophene)s and poly(*para*-phenylene)s, these requirements can be met using KCTCP, a living chain-growth polymerization method based on the formation of an associative pair consisting of the catalytic Ni- or Pd-complex and a growing polymer chain during the entire polymerization, preventing transfer or termination [33–35].

Despite lots of research on Ni-catalyzed KCTCP, still some observations remain unexplained. For instance, when synthesizing poly(*para*-phenylene)-*b*-poly(thiophene) block copolymers via successive monomer addition in Ni-based KCTCP, control over the polymerization is only obtained when polymerizing the *para*-phenylene block first [36]. When reversing the order of monomer addition, hence adding the *para*-phenylene monomer to the living poly(thiophene) block, it is believed that the catalyzing Ni-entity is rather associated with a stronger π-donating thiophene unit, than to ring-walk across an added phenylene unit and subsequently oxidatively initiate at the terminal C-Br bond and thus preventing the polymerization of the second *para*-phenylene block. [21,37] On the other hand, the polymerization of a thiophene-phenylene biaryl monomer via Ni-based KCTCP is reported to occur in a controlled manner [38]. In contrast to the earlier assumption, these findings suggest that a single thiophene unit is not capable of trapping the propagating Ni-complex and that the KCTCP cycle of successive transmetalation (TM), reductive elimination (RE), formation of an associated pair and oxidative addition (OA) is unhindered.

We hypothesize that not one, but several thiophene units contribute

Abbreviations: CTCP, catalyst transfer condensative polymerization; KCTCP, Kumada catalyst transfer condensative polymerization; $\bar{M}_n$, number-average molar mass; GPC, gel permeation chromatography; GRIM, Grignard metathesis; *i*-Pr, isopropyl; THF, tetrahydrofuran; MALDI-ToF, matrix-assisted laser desorption/ionization time-of-flight; NMR, Nuclear Magnetic Resonance; MeOH, methanol; dppp, bisdiphenylphosphinopropane; DP, degree of polymerization; TM, transmetalation; RE, reductive elimination; OA, oxidative addition; PP, *para*-phenylene; PPP, poly(*para*-phenylene)

* Corresponding author.
E-mail address: guy.koeckelberghs@kuleuven.be (G. Koeckelberghs).

https://doi.org/10.1016/j.eurpolymj.2019.109311
Received 17 September 2019; Received in revised form 15 October 2019; Accepted 17 October 2019
Available online 18 October 2019
0014-3057/

to trapping the Ni-entity and set out to investigate this in more detail. If found correct, these insights could hugely impact computational studies on this subject, for mostly only one or two thiophene units are taken into account for these simulations [39–43]. Further, the controlled polymerization of the biaryl monomer shows that it is possible for the Ni-complex to take part in a KCTCP cycle after traversing a *para*-phenylene unit and thus the question rises whether TM, RE and OA are totally absent or only improbable when adding the *para*-phenylene monomer to the living poly(thiophene) block.

To test these hypotheses, we first study to which extend the synthesis of poly(thiophene)-*b*-poly(*para*-phenylene) is obstructed when first polymerizing the thiophene monomer by varying the ratio of *para*-phenylene monomer concentration over the active chain end concentration. Secondly, we investigate the influence of two successive thiophene units on the controlled character of Ni-based KCTCP by polymerizing a thiophene-phenylene-thiophene triaryl monomer. Finally, we study the influence of the length of a thiophene oligomer on the polymerization of a second poly(*para*-phenylene) block during the synthesis of poly(thiophene)-*b*-poly(*para*-phenylene) by successive monomer addition via KCTCP.

2. Results and discussion

First, the influence of the ratio of the 1-bromo-4-chloromagnesio-2,5-dioctyloxybenzene *para*-phenylene monomer **1b** concentration over the active chain end concentration on the formation of poly(thiophene)-*b*-poly(*para*-phenylene) via KCTCP is investigated (Fig. 1). For this, 2-bromo-5-chloromagnesio-3-hexylthiophene **2b** is polymerized using an external *o*-tol. initiator **3b**. After the formation of this living poly (thiophene) block, various volumes of **1b** are added. The obtained polymers are analyzed using standard GPC and ^{1}H NMR spectroscopy [44].

Synthesis of the precursor initiator and monomers. The external *o*-tol. Ni-precursor initiator **3a** is synthesized via the insertion of Ni $(PPh_3)_4$ into the corresponding functionalized aryl bromide, according to literature procedure. [45] The synthesis of the precursor monomers is also conducted as reported in literature [46,47].

Synthesis of the polymers. The polymers are synthesized similar to known procedures. [45] The precursor monomers **1a** and **2a** are converted to the monomers **1b** and **2b** in two separate Grignard metathesis (GRIM) reactions, induced by 1 eq. of *i*-propylmagnesium chloride.lithiumchloride (*i*-PrMgCl.LiCl) in dry THF. Parallel with these GRIM reactions, the precursor initiator **3a** undergoes a ligand exchange

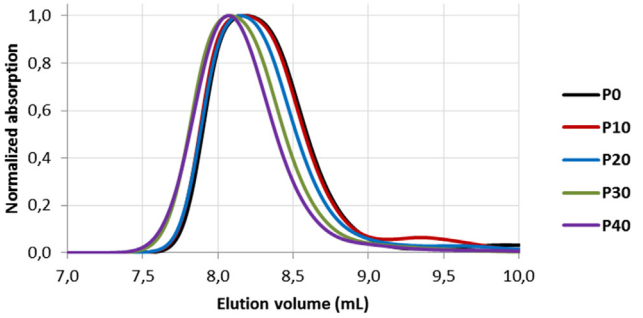

Fig. 2. GPC chromatograms of the raw polymerization mixtures after termination (λ = 440 nm).

with 2 eq. of 1,3-bis(diphenylphosphino)propane (dppp) in dry THF. After completion, the thiophene monomer solution **2b** is cannulated to the initiator solution and the polymerization mixture is left stirring at room temperature. After full conversion, equal volumes of the polymerization mixture are cannulated to different polymerization tubes, after which different volumes of the phenylene monomer solution **1b** are added. In other words, to the living thiophene block comprising of about 17 units (determined via ^{1}H NMR [48], v.i.), 0, 10, 20, 30 and 40 eq. (with respect to the initiator) of **1b** are added to obtain polymers **P0**, **P10**, **P20**, **P30** and **P40**, respectively. Finally, the polymerization is terminated by adding HCl in THF (Fig. 1). For the ^{1}H NMR measurements, the polymers were fractionated using methanol and chloroform to remove quenched monomer and other impurities. Of each GRIM reaction, a small quench with D_2O is taken and analyzed via ^{1}H NMR to verify that the conversion was indeed quantitative.

The GPC chromatograms and results of the raw polymerization mixtures after termination are shown in Fig. 2 and Table 1. Measuring at 440 nm, the λ_{max} region of poly(thiophene), has the advantage of not detecting the residual monomers, resulting in more clear chromatograms.

The ^{1}H NMR spectra and results of polymers **P0**-**P40** after purification are shown in Fig. 3. The presence of only one triplet at 2.61 ppm and not at 2.54 ppm indicates that **P0** is mainly hydrogen terminated and therefore the first poly(thiophene) block was living upon addition of the second, *para*-phenylene, monomer. [48] For polymers **P10** to **P40** the appearance of an extra triplet around 2.55 ppm confirms the chain extension with PP monomer as this triplet most likely originates from the *α*-methylene of a thiophene unit coupled

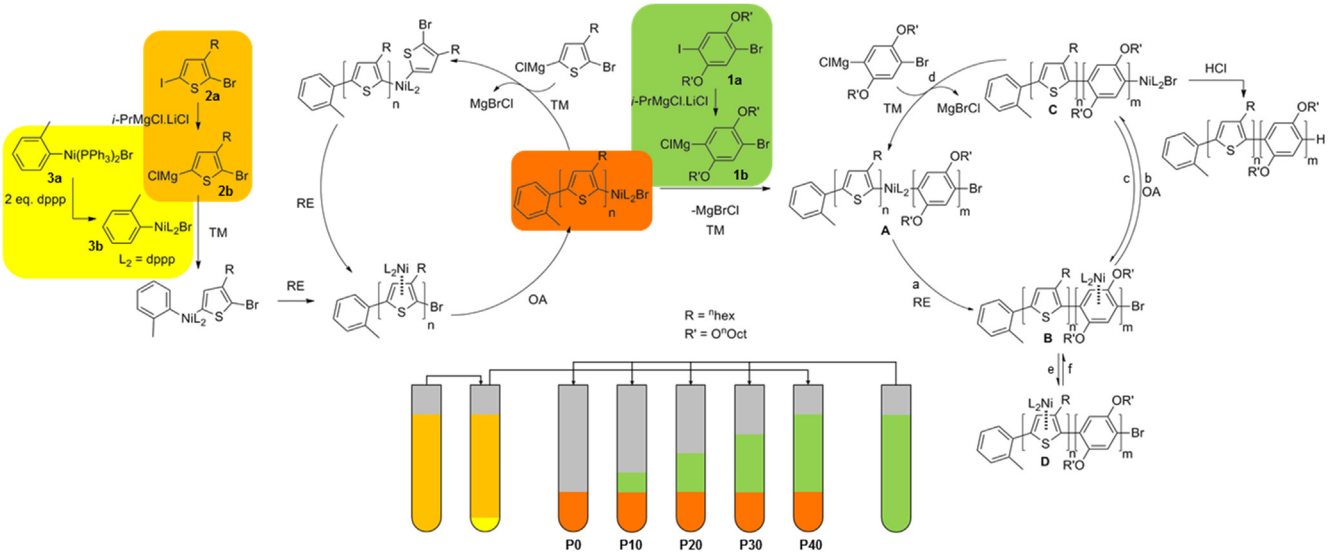

Fig. 1. The (precursor) monomers and initiator and the reaction scheme of the block copolymerization.

Table 1
GPC results of the raw polymerization mixtures.

	M_n (kg/mol)	Đ
P0	2.7	1.1
P10	2.8	1.1
P20	2.9	1.1
P30	3.2	1.1
P40	3.3	1.1

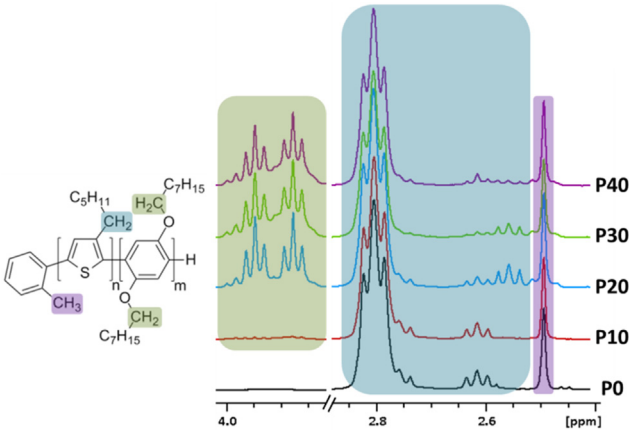

Fig. 3. ^{1}H NMR spectra of polymers **P0-P40** after purification ($CDCl_3$, 400 MHz).

with a *para*-phenylene unit. If this triplet would originate from bromine terminated polymer chains, the GPC chromatograms would not be monomodal. The DP of the thiophene block (17 units) can be obtained via analysis of the ^{1}H NMR spectrum of **P0** by integrating the triplet of the internal *α*-methylene protons around 2.8 ppm, the triplet of the terminal *α*-methylene protons at 2.61 ppm and calibrating on the singlet of the methyl protons of the initiator group at 2.55 ppm [48].

The GPC chromatograms show a chain extension for all polymer samples, since only monomodal curves are observed. From the ^{1}H NMR analysis we can conclude that only a small fraction of the available PP monomer **1b** is built in since the integration of the corresponding NMR regions (between 4.0 and 3.8 ppm) only accord for 0.4 (3.7% yield), 0.7 (3.4% yield), 3.9 (13.0% yield) and 5.1 (12.7% yield) PP-units for **P10**, **P20**, **P30** and **P40**, respectively. Also, the GPC data show that the length of the PPP block increases only slightly with increasing amount of **1b** with respect to the active chain ends. These findings are confirmed by MALDI-ToF measurements, where peaks at higher molar masses appear for polymers **P10** to **P40** (ESI). Further detailed analysis of the MALDI-ToF spectra of the copolymers proves difficult since the molar mass of a *para*-phenylene unit is exactly double the molar mass of a thiophene unit. We conclude that after the addition of the PP monomer resulting in state **C**, there is an equilibrium between propagation (**d**-**a**-**b**) and ringwalking to state **D** (via **c** and **e**) where the Ni-entity is associated with the thiophene block (Fig. 1). With increasing amount of PP monomer compared to the active chain ends, this equilibrium shift slightly to the fast incorporation of the PP monomer, but ultimately the Ni-catalyst migrates to the thiophene block to be permanently trapped in state **D**, terminating the block copolymerization.

Next, in search for more insight in the parameters limiting this thiophene-*para*-phenylene block copolymerization, we performed the KCTCP of a thiophene-phenylene-thiophene based triaryl monomer to investigate whether or not the polymerization is hindered by the Ni-catalyst interacting with two successive thiophene units and to which extend the polymerization is controlled. For this, 1-(5-bromo-2-thienyl)-4-(5-iodo-2-thienyl)-2,5-di-(2-octyldodecyloxy)benzene **I-Th-PP-Th-Br** is polymerized using Ni-catalyst **3b** in a series with increasing monomer over initiator concentration. The bulky octyldodecyl side chains were chosen to ensure solubility.

Synthesis of the precursor monomer. The synthesis of **I-Th-PP-Th-Br** is depicted in Fig. 4 and starts with the formation of 2-octyldodecyl bromide by an Apple reaction for the subsequent alkylation of hydroquinone. After diiodination and double coupling with 2-thiopheneboronic acid through a Suzuki reaction, the subsequent bromination and iodination yielded the **I-Th-PP-Th-Br** precursor monomer.

Synthesis of the polymer. First the GRIM reaction of the **I-Th-PP-Th-Br** precursor monomer to the **ClMg-Th-PP-Th-Br** monomer and the polymerization conditions were optimized. It was found that a quantitative GRIM reaction was obtained with 1 eq. of *i*-PrMgCl.LiCl at 0 °C in dry THF after 30 min. To initiate the polymerization, the monomer solution is cannulated to solutions of **3b** in dry THF, as described earlier. At regular time intervals quenches of the polymerization mixture in

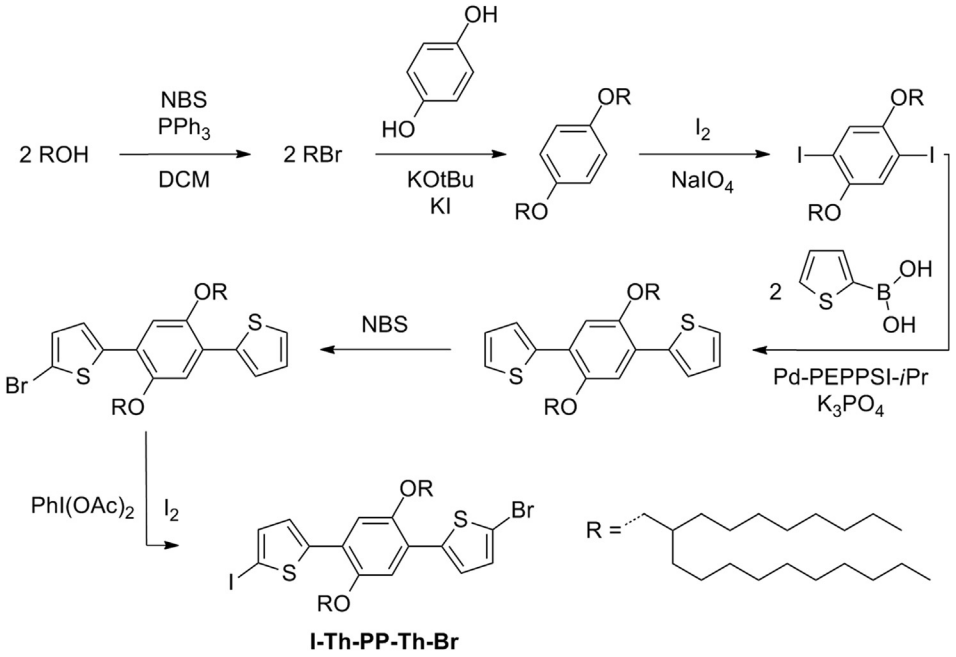

Fig. 4. The synthesis of the **I-Th-PP-Th-Br** precursor monomer.

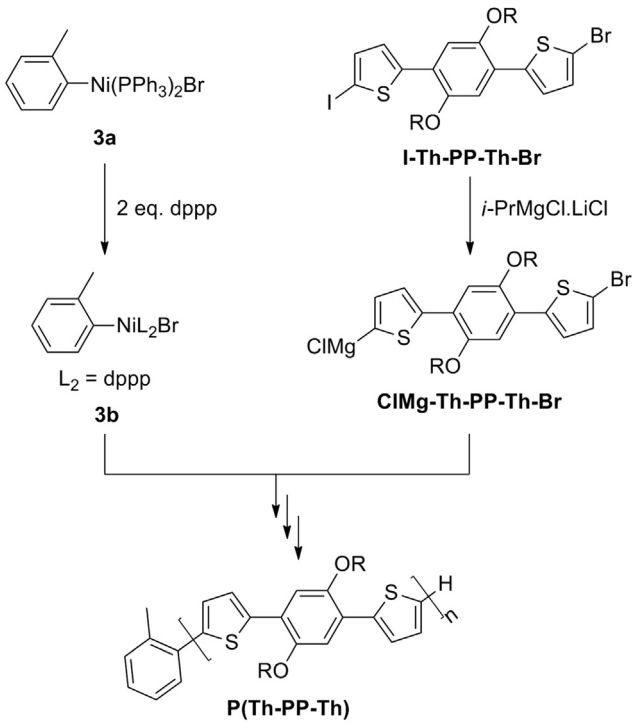

Fig. 5. The synthesis of the **P(Th-PP-Th-Br)** polymers.

Table 2
GPC results of the raw polymerization mixtures after termination and the GPC-determined M_n plotted over the initial monomer concentration ($[M]_0$) divided by the initiator concentration ($[I]$).

	$[M]_0/[I]$	M_n (kg/mol)	Đ
P(Th-PP-Th)8.3	8.3	11.2	1.2
P(Th-PP-Th)13.9	13.9	15.3	1.4
P(Th-PP-Th)19.4	19.4	17.9	1.4
P(Th-PP-Th)25.0	25.0	21.6	1.4
P(Th-PP-Th)37.5	37.5	22.3	1.4
P(Th-PP-Th)56.3	56.3	22.5	1.4

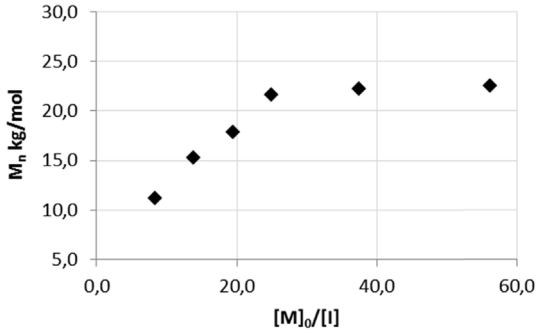

Fig. 6. GPC results of the raw polymerization mixtures after termination and the GPC-determined M_n plotted over the initial monomer concentration ($[M]_0$) divided by the initiator concentration ($[I]$).

D_2O were taken and analyzed using ^1H NMR. After full conversion, the polymerization was terminated by the addition of HCl in THF (Fig. 5). These optimized polymerization conditions were then used in the following experiments to ensure a full conversion. **P(Th-PP-Th)** was synthesized in a series with increasing monomer over initiator concentration: $[M]_0/[I]$ = 8.3, 13.9, 19.4, 25.0, 37.5 and 56.3 to form **P(Th-PP-Th)8.3**, **P(Th-PP-Th)13.9**, **P(Th-PP-Th)19.4**, **P(Th-PP-Th)25.0**, **P(Th-PP-Th)37.5** and **P(Th-PP-Th)56.3** respectively. The GPC results of the raw polymerization mixtures after termination are shown in and Table 2. Monomodal curves of the polymer materials are observed. The GPC-determined M_n is plotted over the initial monomer concentration ($[M]_0$) divided by the initiator concentration ($[I]$) (Fig. 6). For a controlled polymerization, where transfer and termination reactions are absent, a linear relation between these quantities is expected. Indeed, a linear relation is observed until 22 kg/mol after which the curve flattens out, indicating termination reactions. From the obtained GPC results we can conclude that the polymerization of the **I-Th-PP-Th-Br** monomer is controlled until 22 kg/mol, showing that the Ni-catalyst is not hindered by two successive thiophene units.

We proved that the Ni-catalyst is not irreversibly associated with two consecutive thiophene units and can even transverse an adjacent phenyl unit to allow polymerization, which was not the case for a thiophene block consisting of multiple thiophene units. Next, we investigate how many thiophene units it takes to disrupt the formation of poly(thiophene)-*b*-poly(*para*-phenylene) by systematically lengthening the thiophene block from 4 to 6 and 8 thiophene units.

Synthesis of the precursor monomers. The syntheses of the precursor monomers is conducted as reported in literature [47,48].

Synthesis of the polymers. The polymerization experiment is conducted similar to what is earlier described. The precursor monomers **1a** and **2a** are converted to the monomers **1b** and **2b** in two separate GRIM reactions. After completion, equal volumes of the thiophene monomer solution **2b** are cannulated to several initiator solutions and the polymerization mixture is left to stir at room temperature. After full conversion, half the polymerization mixtures are cannulated into a HCl solution in THF for termination to obtain polymers **P4Th**, **P6Th** and **P8Th**, respectively. Next, the phenylene monomer solution **1b** is added: 36 eq. with respect to the initiator to synthesize block copolymers **P4ThPP**, **P6ThPP** and **P8ThPP** respectively. Finally, the polymerization is terminated by adding HCl in THF.

The GPC chromatograms and results of the raw polymerization mixtures after termination are shown in Fig. 7 and Table 3, respectively. Fig. 8 shows a visual representation of the data in Table 3. The bimodal shape of the **P6ThPP** curve can be explained by the first block being partially dead before the addition of the second monomer. The length of the *para*-phelylene blocks **PP** in the **PXThPP** polymers is calculated by subtraction of the molar masses of the **PXTh** homopolymers **Th** from the molar masses of the block-copolymers **ThPP**. We note that this reasoning in not fully accurate since the GPC calibration curves for poly(thiophene) and poly(*para*-phenylene) differ, but either way, the observed trend is credible enough to make a qualitative conclusion. The results show that the longer the first thiophene block, the shorter the second *para*-phenylene block is. The polymerization of the *para*-phenylene block seems to be more hindered with increasing thiophene units in the first block, suggesting that the Ni-catalyst is only

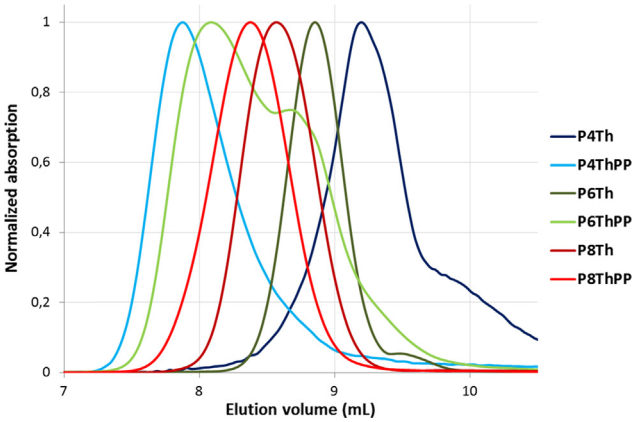

Fig. 7. GPC chromatograms of the raw polymerization mixtures of **P4Th**, **P6Th**, **P8Th**, **P4ThPP**, **P6ThPP** and **P8ThPP** after termination (λ = 440 nm).

Table 3
Molar masses (kg/mol) of polymers **P4Th**, **P6Th**, **P8Th**, **P4ThPP**, **P6ThPP** and **P8ThPP** and the calculated (**ThPP** - **Th**) molar masses of the poly(*para*-phenylene) block (**PP**).

	Th	ThPP	PP
P4	1.9	20.3	18.4
P6	3.4	13.9	10.5
P8	5.8	8.2	2.4

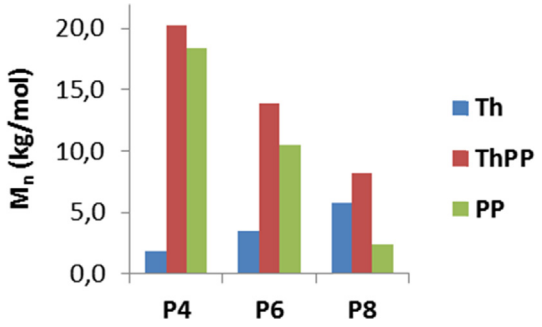

Fig. 8. Molar masses (kg/mol) of polymers **P4Th**, **P6Th**, **P8Th**, **P4ThPP**, **P6ThPP** and **P8ThPP** and the calculated (ThPP - Th) molar masses of the poly (*para*-phenylene) block (PP).

substantially associated with the first block if this block consist of more than four sequential thiophene units. This supports our hypothesis that it is in fact an oligothiophene that strongly interacts with the Ni-catalyst and not just two or three thiophene units. In other words, there exist an equilibrium (**e**, **f**) between states **B** and **D** (Fig. 1), for which it holds that the ratio **e** over **f** increases with increasing degree of polymerization of the thiophene block. When the thiophene block is sufficiently long enough, route **f** becomes negligible and the Ni-entity is permanently associated with the thiophene block, hindering further polymerization.

The right hand side of Fig. 1 summarizes all previous results. When synthesizing poly(thiophene)-*b*-poly(*para*-phenylene) via successive addition of an excess of the *para*-phenylene (PP) monomer to the living poly(thiophene) block using KCTCP, all polymer chains are slightly elongated. We conclude that there is a balance between propagation and association with the thiophene block. With increasing amount PP monomer with respect to the active chain ends, this equilibrium shift slightly to the fast incorporation of the PP monomer resulting in a longer poly(*para*-phenylene) block, but ultimately the Ni-catalyst migrates to the thiophene block to be permanently trapped, terminating the block copolymerization.

Further, by polymerizing a thiophene-phenylene-phenylene triaryl monomer, the Ni-catalyst is not hindered by two successive thiophene units.

Finally, we show that for the synthesis of poly(thiophene)-*b*-poly(*para*-phenylene) via successive monomer addition in Ni-based KCTCP, the longer the first thiophene block, the shorter the second *para*-phenylene block is. The polymerization of the *para*-phenylene is more hindered with increasing thiophene units in the first block, suggesting that the Ni-catalyst is only substantially associated with the first block if this block consist of more than four sequential thiophene units. This supports our hypothesis that it is in fact an oligothiophene, that strongly interact with the Ni-catalyst and not just two or three thiophene units. On the molecular level this would mean that the association of the nickel complex comprises not the orbitals of one thiophene unit, but rather the molecular orbitals of an extended oligothiophene. These insights could impact computational studies on the subject, for mostly only one or two thiophene units are taken into account for these simulations.

3. Conclusion

To summarize we demonstrated that when adding a *para*-phenylene monomer to a living thiophene block to synthesize poly(thiophene)-*b*-poly(*para*-phenylene) using Ni-based KCTCP, an equilibrium exist between the incorporation of the PP monomer and the trapping of the Ni-catalyst by association with the thiophene block. We suggest that this equilibrium shifts toward the association with increasing length of the thiophene block and that significant trapping only occurs when this block consist of several thiophene units. Also, the more PP monomers already built in, the more likely it becomes that the Ni-catalyst will have ringwalked to the thiophene block instead of incorporating another PP monomer. These findings contribute to a more complete understanding of KCTCP, necessary for the controlled synthesis of new materials for high-end future applications.

4. Notes

The authors declare no competing financial interest.

Declaration of Competing Interest

There is no conflict of interest.

Acknowledgment

We are grateful to the Onderzoeksfonds KU Leuven/Research Fund KU Leuven, IWT-SBO and the Fund for Scientific Research (FWO Vlaanderen) for financial support. W.C. is grateful to IWT for a doctoral fellowship. The UMONS MS laboratory acknowledges the Fonds National de la Recherche Scientifique (FRS-FNRS) for its contribution to the acquisition of the Waters QToF Premier mass spectrometer and for continuing support.

Appendix A. Supplementary material

Used instrumentation and experimental details as well as ^{1}H NMR, GPC chromatograms and MALDI-ToF spectra. Supplementary data to this article can be found online at https://doi.org/10.1016/j.eurpolymj.2019.109311.

References

[1] P.M. Beaujuge, J.M.J. Fréchet, Molecular design and ordering effects in π-functional materials for transistor and solar cell applications, J. Am. Chem. Soc. 133 (50) (2011) 20009–20029, https://doi.org/10.1021/ja2073643.
[2] J. Shinar (Ed.), Organic Light-Emitting Devices, Springer New York, New York, NY, 2004.
[3] Y.J. Cheng, S.H. Yang, C.S. Hsu, Synthesis of conjugated polymers for organic solar cell applications, Chem. Rev. 109 (11) (2009) 5868–5923, https://doi.org/10.1021/cr900182s.
[4] A.C. Grimsdale, K. Leok Chan, R.E. Martin, P.G. Jokisz, A.B. Holmes, Synthesis of light-emitting conjugated polymers for applications in electroluminescent devices, Chem. Rev. 109 (3) (2009) 897–1091, https://doi.org/10.1021/cr000013v.
[5] M.E. Roberts, A.N. Sokolov, Z. Bao, Material and device considerations for organic thin-film transistor sensors, J. Mater. Chem. 19 (21) (2009) 3351–3363, https://doi.org/10.1039/b816386c.
[6] I.F. Perepichka, D.F. Perepichka (Eds.), Handbook of Thiophene-Based Materials, John Wiley & Sons, Ltd, Chichester, UK, 2009.
[7] T. Someya, A. Dodabalapur, J. Huang, K.C. See, H.E. Katz, Chemical and physical sensing by organic field-effect transistors and related devices, Adv. Mater. 22 (34) (2010) 3799–3811, https://doi.org/10.1002/adma.200902760.
[8] P.L.T. Boudreault, A. Najari, M. Leclerc, Processable low-bandgap polymers for photovoltaic applications, Chem. Mater. 23 (3) (2011) 456–469, https://doi.org/10.1021/cm1021855.
[9] A. Facchetti, π-conjugated polymers for organic electronics and photovoltaic cell applications, Chem. Mater. 23 (3) (2011) 733–758, https://doi.org/10.1021/cm102419z.
[10] P. Lin, F. Yan, Organic thin-film transistors for chemical and biological sensing, Adv. Mater. 24 (1) (2012) 34–51, https://doi.org/10.1002/adma.201103334.
[11] H. Zhou, L. Yang, W. You, Rational design of high performance conjugated polymers for organic solar cells, Macromolecules 45 (2) (2012) 607–632, https://doi.

org/10.1021/ma201648t.
[12] W. Han, M. He, M. Byun, B. Li, Z. Lin, Large-scale hierarchically structured conjugated polymer assemblies with enhanced electrical conductivity, Angew. Chem. - Int. Ed. 52 (9) (2013) 2564–2568, https://doi.org/10.1002/anie.201209632.
[13] J. Mei, Y. Diao, A.L. Appleton, L. Fang, Z. Bao, Integrated materials design of organic semiconductors for field-effect transistors, J. Am. Chem. Soc. 135 (18) (2013) 6724–6746, https://doi.org/10.1021/ja400881n.
[14] J. Jung, X. Pang, C. Feng, Z. Lin, Semiconducting conjugated polymer-inorganic tetrapod nanocomposites, Langmuir 29 (25) (2013) 8086–8092, https://doi.org/10.1021/la400925y.
[15] J. Jung, Y.J. Yoon, M. He, Z. Lin, Organic-inorganic nanocomposites composed of conjugated polymers and semiconductor nanocrystals for photovoltaics, J. Polym. Sci. Part B Polym. Phys. 52 (24) (2014) 1641–1660, https://doi.org/10.1002/polb.23612.
[16] L. Lu, T. Zheng, Q. Wu, A.M. Schneider, D. Zhao, L. Yu, Recent advances in bulk heterojunction polymer solar cells, Chem. Rev. 115 (23) (2015) 12666–12731, https://doi.org/10.1021/acs.chemrev.5b00098.
[17] T.P. Huynh, P.S. Sharma, M. Sosnowska, F. D'Souza, W. Kutner, Functionalized polythiophenes: recognition materials for chemosensors and biosensors of superior sensitivity, selectivity, and detectability, Prog. Polym. Sci. 47 (2015) 1–25, https://doi.org/10.1016/j.progpolymsci.2015.04.009.
[18] G. Zhang, Z.-A. Lan, X. Wang, Conjugated polymers: catalysts for photocatalytic hydrogen evolution, Angew. Chem. Int. Ed. 55 (51) (2016) 15712–15727, https://doi.org/10.1002/anie.201607375.
[19] G. Li, W.H. Chang, Y. Yang, Low-bandgap conjugated polymers enabling solution-processable tandem solar cells, Nat. Rev. Mater. 2 (8) (2017) 1–13, https://doi.org/10.1038/natrevmats.2017.43.
[20] D.T. McQuade, A.E. Pullen, T.M. Swager, Conjugated polymer-based chemical sensors, Chem. Rev. 100 (7) (2000) 2537–2574, https://doi.org/10.1021/cr9801014.
[21] L. Verheyen, P. Leysen, M.-P. Van Den Eede, W. Ceunen, T. Hardeman, G. Koeckelberghs, Advances in the controlled polymerization of conjugated polymers, Polymer (Guildf). 108 (2017) 521–546, https://doi.org/10.1016/j.polymer.2016.09.085.
[22] A. Salleo, R.J. Kline, D.M. DeLongchamp, M.L. Chabinyc, Microstructural characterization and charge transport in thin films of conjugated polymers, Adv. Mater. 22 (34) (2010) 3812–3838, https://doi.org/10.1002/adma.200903712.
[23] K. Vakhshouri, D.R. Kozub, C. Wang, A. Salleo, E.D. Gomez, Effect of miscibility and percolation on electron transport in amorphous poly(3-hexylthiophene)/phenyl-C 61-butyric acid methyl ester blends, Phys. Rev. Lett. 108 (2) (2012), https://doi.org/10.1103/PhysRevLett. 108.026601.
[24] S. Günes, H. Neugebauer, N.S. Sariciftci, Conjugated polymer-based organic solar cells, Chem. Rev. 107 (4) (2007) 1324–1338, https://doi.org/10.1021/cr050149z.
[25] M.T. Dang, L. Hirsch, G. Wantz, P3HT:PCBM, best seller in polymer photovoltaic research, Adv. Mater. 23 (31) (2011) 3597–3602, https://doi.org/10.1002/adma.201100792.
[26] P. Sista, C.K. Luscombe, Progress in the Synthesis of Poly (3-Hexylthiophene), 2014, pp 1–38.
[27] A. Marrocchi, D. Lanari, A. Facchetti, L. Vaccaro, Poly(3-hexylthiophene): synthetic methodologies and properties in bulk heterojunction solar cells, Energy Environ. Sci. 5 (9) (2012) 8457, https://doi.org/10.1039/c2ee22129b.
[28] T. Vangerven, P. Verstappen, J. Drijkoningen, W. Dierckx, S. Himmelberger, A. Salleo, D. Vanderzande, W. Maes, J.V. Manca, Molar mass versus polymer solar cell performance: highlighting the role of homocouplings, Chem. Mater. 27 (10) (2015) 3726–3732, https://doi.org/10.1021/acs.chemmater.5b00939.
[29] M.P. Aplan, E.D. Gomez, Recent developments in chain-growth polymerizations of conjugated polymers, Ind. Eng. Chem. Res. 56 (28) (2017) 7888–7901, https://doi.org/10.1021/acs.iecr.7b01030.
[30] T. Yokozawa, Y. Ohta, Transformation of step-growth polymerization into living chain-growth polymerization, Chem. Rev. 116 (4) (2016) 1950–1968, https://doi.org/10.1021/acs.chemrev.5b00393.
[31] C. Lee, S. Lee, G.-U. Kim, W. Lee, B.J. Kim, Recent advances, design guidelines, and prospects of all-polymer solar cells, Chem. Rev. 119 (13) (2019) 8028–8086, https://doi.org/10.1021/acs.chemrev.9b00044.
[32] J. Wang, T. Higashihara, Synthesis of all-conjugated donor-acceptor block copolymers and their application in all-polymer solar cells, Polym. Chem. 4 (22) (2013) 5518, https://doi.org/10.1039/c3py00979c.
[33] Z.J. Bryan, A.J. McNeil, Conjugated polymer synthesis via catalyst-transfer polycondensation (CTP): mechanism, scope, and applications, Macromolecules 46 (21) (2013) 8395–8405, https://doi.org/10.1021/ma401314x.
[34] R.D. McCullough, C.O.N. Spectus, I. Osaka, R.D. McCullough, Advances in molecular design and synthesis of regioregular polythiophenes, Acc. Chem. Res. 41 (9) (2008) 1202–1214, https://doi.org/10.1021/ar800130s.
[35] M. Leclerc, J.-F. Morin (Eds.), Design and Synthesis of Conjugated Polymers, Wiley-VCH Verlag GmbH & Co. KGaA, Weinheim, Germany, 2010.
[36] R. Miyakoshi, A. Yokoyama, T. Yokozawa, Importance of the order of successive catalyst-transfer condensation polymerization in the synthesis of block copolymers of polythiophene and poly(p-phenylene), Chem. Lett. 37 (10) (2008) 1022–1023, https://doi.org/10.1246/cl.2008.1022.
[37] R. Miyakoshi, K. Shimono, A. Yokoyama, T. Yokozawa, Catalyst-transfer polycondensation for the synthesis of poly(p-phenylene) with controlled molecular weight and low polydispersity, J. Am. Chem. Soc. 128 (50) (2006) 16012–16013, https://doi.org/10.1021/ja067107s.
[38] R.J. Ono, S. Kang, C.W. Bielawski, Controlled Chain-Growth Kumada catalyst transfer polycondensation of a conjugated alternating copolymer, Macromolecules 45 (5) (2012) 2321–2326, https://doi.org/10.1021/ma300013e.
[39] K. Mikami, M. Nojima, Y. Masumoto, Y. Mizukoshi, R. Takita, T. Yokozawa, M. Uchiyama, Catalyst-dependent intrinsic ring-walking behavior on π-face of conjugated polymers, Polym. Chem. 8 (10) (2017) 1708–1713, https://doi.org/10.1039/c6py01934j.
[40] N. Bahri-Laleh, A. Poater, L. Cavallo, S.A. Mirmohammadi, Exploring the mechanism of grignard metathesis polymerization of 3-alkylthiophenes, Dalt. Trans. 43 (40) (2014) 15143–15150, https://doi.org/10.1039/c4dt01617c.
[41] J.A. Bilbrey, S.K. Sontag, N.E. Huddleston, W.D. Allen, J. Locklin, On the role of disproportionation energy in Kumada catalyst-transfer polycondensation, ACS Macro Lett. 1 (8) (2012) 995–1000, https://doi.org/10.1021/mz3002929.
[42] J.A. Bilbrey, A.N. Bootsma, M.A. Bartlett, J. Locklin, S.E. Wheeler, W.D. Allen, Ring-walking of zerovalent nickel on aryl halides, J. Chem. Theory Comput. 13 (4) (2017) 1706–1711, https://doi.org/10.1021/acs.jctc.6b01143.
[43] S.K. Sontag, J.A. Bilbrey, N.E. Huddleston, G.R. Sheppard, W.D. Allen, J. Locklin, Π-complexation in nickel-catalyzed cross-coupling reactions, J. Org. Chem. 79 (4) (2014) 1836–1841, https://doi.org/10.1021/jo402259z.
[44] F. Monnaie, W. Brullot, T. Verbiest, J. De Winter, P. Gerbaux, A. Smeets, G. Koeckelberghs, Synthesis of end-group functionalized P3HT: general protocol for P3HT/nanoparticle hybrids, Macromolecules 46 (21) (2013) 8500–8508, https://doi.org/10.1021/ma401809e.
[45] A. Smeets, K. Van den Bergh, J. De Winter, P. Gerbaux, T. Verbiest, G. Koeckelberghs, Incorporation of different end groups in conjugated polymers using functional nickel initiators, Macromolecules 42 (20) (2009) 7638–7641, https://doi.org/10.1021/ma901888h.
[46] K. Van den Bergh, J. Huybrechts, T. Verbiest, G. Koeckelberghs, Transfer of supramolecular chirality in block copoly(thiophene)s, Chemistry 14 (30) (2008) 9122–9125, https://doi.org/10.1002/chem.200801537.
[47] H.C. Lin, M. Shellaiah, M.V. Ramakrishnam Raju, A. Singh, H.C. Lin, K.H. Wei, Synthesis of novel platinum complex core as a selective Ag+sensor and Its H-bonded tetrads self-assembled with triarylamine dendrimers for electron/energy transfers, J. Mater. Chem. A 2 (41) (2014) 17463–17476, https://doi.org/10.1039/c4ta04231j.
[48] V. Senkovskyy, N. Khanduyeva, H. Komber, U. Oertel, M. Stamm, D. Kuckling, A. Kiriy, Conductive polymer brushes of regioregular head-to-tail poly(3-alkylthiophenes) via catalyst-transfer surface-initiated polycondensation, J. Am. Chem. Soc. 129 (20) (2007) 6626–6632, https://doi.org/10.1021/ja0710306.